

# Visual Alignment of Medical Vision-Language Models for Grounded Radiology Report Generation

Sarosij Bose<sup>1,2</sup> <sup>†</sup>, Ravi K. Rajendran<sup>1</sup>, Biplob Debnath<sup>1</sup>, Konstantinos Karydis<sup>2</sup>  
Amit K. Roy-Chowdhury<sup>2</sup>, Srimat T. Chakradhar<sup>1</sup>

<sup>1</sup>NEC Laboratories America

<sup>2</sup>University of California, Riverside

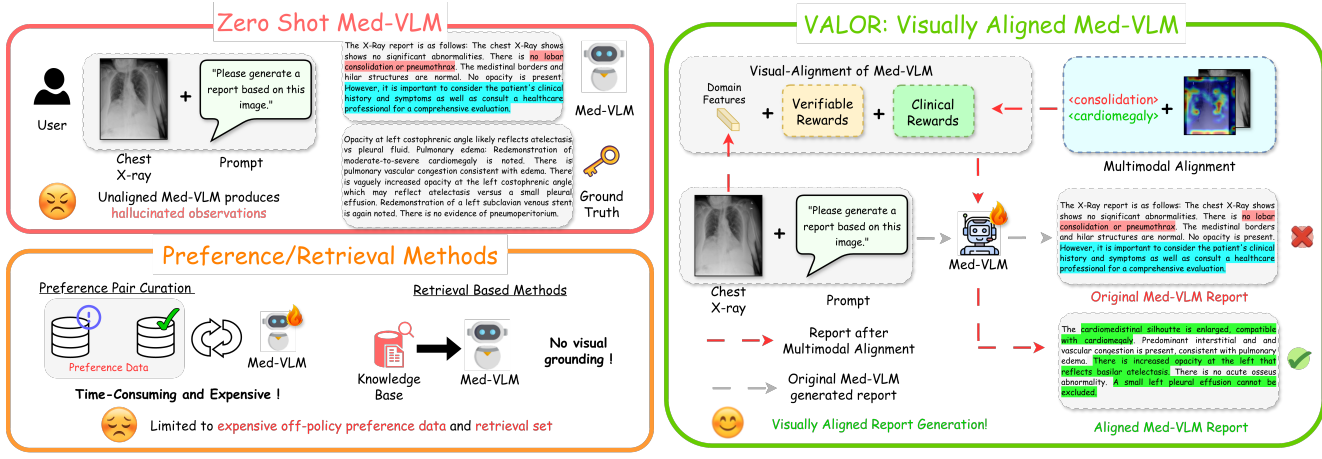


Figure 1. **Overview:** We introduce **VALOR**, a multimodal alignment framework that addresses the visual hallucinations of existing Med-VLMs [27]. **Left:** the generated response from vanilla Med-VLM where the misalignment with the input image is marked in **red** and generic non-medical text in **cyan**. Existing approaches resort to the curation of preference data per-task or on retrieval of reports which is inherently time-consuming and does not address the issue of multimodal alignment. **Right:** Our proposed **VALOR** addresses this issue with a novel visual reasoning based pipeline which utilizes multi-modal rewards for optimization and pushes the model to generate more clinical informed and grounded reports aligned with the original image which are marked in **green**.

## Abstract

*Radiology Report Generation (RRG) is a critical step toward automating healthcare workflows, facilitating accurate patient assessments, and reducing the workload of medical professionals. Despite recent progress in Large Medical Vision-Language Models (Med-VLMs), generating radiology reports that are both visually grounded and clinically accurate remains a significant challenge. Existing approaches often rely on large labeled corpora for pre-training, costly task-specific preference data, or retrieval-based methods. However, these strategies do not adequately mitigate hallucinations arising from poor cross-modal alignment between visual and linguistic representations. To address these limitations, we propose **VALOR**: Visual Alignment of Medical Vision-Language Models for GrOunded Radiology Report Generation. Our method in-*

*troduces a reinforcement learning-based post-alignment framework utilizing Group-Relative Proximal Optimization (GRPO). The training proceeds in two stages: (1) improving the Med-VLM with textual rewards to encourage clinically precise terminology, and (2) aligning the vision projection module of the textually grounded model with disease findings, thereby guiding attention toward image regions most relevant to the diagnostic task. Extensive experiments on multiple benchmarks demonstrate that **VALOR** substantially improves factual accuracy and visual grounding, achieving significant performance gains over state-of-the-art report generation methods.*

## 1. Introduction

Radiology reports constitute a fundamental component of assistive diagnosis, serving as a structured medium through which complex visual findings in X-ray images are translated into clinically actionable insights. By standardizing

<sup>†</sup>Work done as an intern at NEC Laboratories

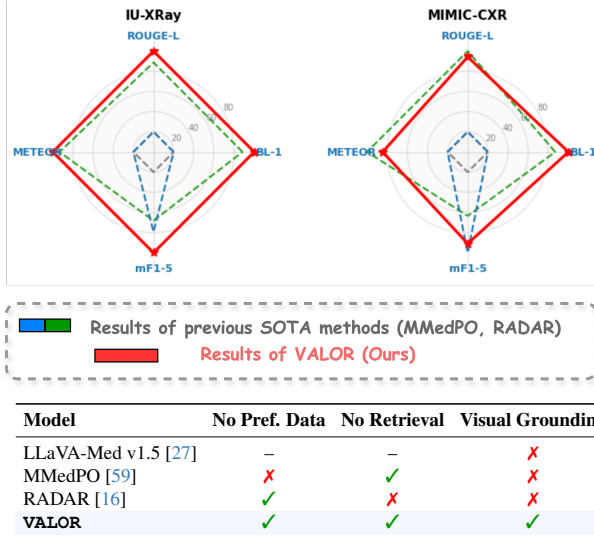


Figure 2. **Comparison with SOTA methods.** VALOR performs significantly better in both generation [13, 30, 34] and clinical metrics [22, 41] compared to preference-data and retrieval-based methods. Further, they don’t account for visual grounding w.r.t the input image as shown in the table.

the description of anatomical regions and pathological observations, these reports not only enable more efficient and consistent patient assessment but also alleviate the cognitive and administrative burdens on healthcare professionals.

Preparing chest X-ray reports requires deep clinical and anatomical expertise to visually identify disease-relevant regions and accurately describe them. This burden has motivated the development of automated chest X-ray report generation techniques, largely driven by the rise of Large Medical Vision-Language Models (Med-VLMs) [27, 33, 39, 56, 57]. However, improving cross-modal alignment [1, 5, 58]—that is, the ability to explicitly associate radiological findings with corresponding X-ray regions, and thereby *ground* generated reports—is critical to ensure that these reports contain image-relevant disease findings. Failure to do so results in “Visual Hallucinations” stemming from the inherent tendency of these models to generate information from their reliance on a text-heavy pre-training corpus [18, 25, 31] and using retrieval-augmented pipelines that may incorporate disease statements from retrieved reports even when unsupported by the image [16, 51] bypassing actual multimodal reasoning [7] needed for explainability of report generation systems, as shown in Figure 1.

To mitigate these challenges, existing efforts can be broadly divided into two categories: 1) *Construction of high-quality medical preference datasets*: either by leveraging expert preferences [6, 11] or by constructing additional data generation and training pipelines requiring significant time and extra computational resources [59]. While promising, these methods remain overly sensitive to the quality of preference data, often

generated using simplistic techniques such as random masking or additive noise, which may result in loss of information and, most importantly, fail to explicitly enforce that generated reports are grounded in the input X-ray. 2) *Domain Knowledge Retrieval*: by either training domain-specific retrievers or curating retrieval knowledge bases [16, 42, 51]. However, the scarcity of such external multimodal medical knowledge, the inherent semantic gap between retrieved reports and medical images, and the limited scope of the retrieval set all lead to ineffective visual grounding as reflected in NLG and Clinical Metrics [13, 30, 34, 41] (Figure 2). These prompts us to ask the question: *Can we design a framework that generates clinically informative reports which are both factually accurate and visually grounded in the image?*

To address these challenges, we propose **VALOR**: *Visual Alignment of Medical Vision-Language Models for GrOunded Radiology Report Generation*, a post-training alignment framework that improves the medical reasoning of Med-VLMs with both textual and visual rewards to reduce hallucinations and strengthen image-report consistency. Our *main contributions* are **threefold**:

- **Multi-Stage Alignment.** We introduce a novel multi-stage reinforcement learning-based pipeline, where the base Med-VLM [27] is aligned in the *textual* space and then refined for *visual* alignment. In the first stage, we craft textual rewards with natural language metrics BLEU [34], ROUGE [30], BERTScore [55] for semantic completeness, and clinical metrics CheXbert [41] and RadGraph [22] for clinical guidance, with format consistency rewards. In the second stage, we utilize multi-label features to compute *image-text similarity scores*, explicitly steering the model towards disease-relevant regions.
- **Hybrid Reward Formulation for Reasoning.** To achieve multimodal medical reasoning, our novel multi-stage reward regimen blends commonly used NLG and Clinical metrics as rewards to supervise the model with enriched medical terminology. We then use normalized image-text similarity scores between domain features from a disease classifier [21] and generated candidate reports to compute *rank-normalized advantages*, assigning more weightage to reports that are aligned to the image, thus enabling effective visual-text integration.
- **Extensive evaluation on Radiology Report Generation.** We extensively evaluate VALOR on the IU-XRay [12] and MIMIC-CXR [24] datasets across diverse scenarios: generation quality, clinical accuracy and verify that our method achieves effective visual grounding qualitatively. VALOR consistently outperforms preference-based, retrieval-based and SOTA proprietary LLMs producing more faithful reports whose attention maps concentrate on clinically meaningful regions, demonstrating improved factual accuracy and visual alignment.

## 2. Related Works

**Radiology Report Generation (RRG).** Radiology report generation involves composing descriptive sentences that capture the contents of a medical image, organized into a ‘Findings’ section for detailed observations and an Impression section for clinical interpretation. While standard image captioning tasks involve answering in brief, closed-set settings, RRG typically involves generating much larger quantities of text in a precise manner that is clinically informed and aligned with the image. Various works have been proposed along these lines [19, 23, 28].

Existing approaches for RRG can be broadly categorized into three groups. The first focuses on directly improving the encoder-decoder architecture to generate more consistent and medically enriched reports. Earlier approaches used LSTM [15] based networks with hierarchical structures to manage the descriptiveness of radiology reports [44] or dynamic graphs with a contrastive learning paradigm [28]. The second group of approaches focuses on closest report retrieval using retrieval-augmented generation (RAG) techniques, where a retriever is trained based on medical informativeness and targeted retrieval using domain knowledge [10, 14, 29, 50]. RADAR [16] employs the combination of retrieved reports and the overlap with the potential diseases which may be there in the image. However, these methods employ terminology that is misaligned with the image, limiting their reliability in clinical practice.

**Reinforcement Learning in LLMs/VLMs.** Despite the rise of Supervised Fine-Tuning (SFT)-based techniques, Reinforcement Learning (RL)-based approaches have also gained popularity owing to their robustness, scalability, ability to align with human preferences, and ability to mitigate hallucinations [48, 52, 58]. MMedPO [59] utilizes a Direct Preference Optimization (DPO)-based approach based on curating preference data to mitigate hallucinations in Med-VLMs. However, it requires the curation of preference data, which is time-consuming and expensive, and does not generalize well outside of the curated preference data. Our work focuses on addressing this limitation by applying GRPO [40]-based RL using verifiable rewards with a focus on unifying both modalities, which enhances the medical reasoning capabilities of the model.

**Medical Reasoning using Vision Language Models.** With the widespread success of CLIP [36], several other VLMs have arisen in the medical space such as Med-Flamingo [32], BioMedGPT [53] and HuatuoGPT-Vision [6] which learn the cross-modal information across a large scale of pre-training data across various vision and language modalities such as CheXzero [45], Med-CLIP [46] and BioMedCLIP [54] which focus on enhancing the understanding of raw reports with images whereas BioVIL [4], BioVIL-T [2] enhance the encoding of the textual descriptions. More recent work, such as MedKLIP [49]

leverages the spatial relationships from RadGraph [22] to incorporate more fine-grained medical information into the pre-training regimen. DART [35] proposed a self-correcting report generation mechanism that focused on improving both the encoding and decoding processes. Methods such as MMedAgent [26] and VILA-M3 [33] utilize expert knowledge (requiring annotation) and tool usage (prone to model noise) as additional proxies of information for alignment to the medical domain. Thus, these successes can be largely attributed to the availability of a large corpus of labeled pretrained data and largely ignore the alignment of human preferences with the provided image. It is therefore important to move away from external dependencies such as tools, preference data or retrieval datasets and adjust the inherent reasoning focus of the model towards improved clinical accuracy and groundedness to the input X-Ray. *Our novel multi-stage RL-based reasoning pipeline aims to address this open challenge of improving the visual abilities of Med-VLMs without using additional external knowledge.*

## 3. Preliminaries

**Problem Formulation.** Given a 2D chest X-ray image  $\mathcal{I} \in \mathbb{R}^{H \times W \times 3}$ , a textual prompt  $P$ , and a dataset  $\mathcal{D} = \{(\mathcal{I}, \mathcal{R}_{\text{gt}})\}$  of images and ground truth reports, the goal of radiology report generation is to produce a report  $\mathcal{R}$  that is clinically accurate and aligned with the input image  $\mathcal{I}$ . We model this with a base Med-VLM  $\mathcal{M}_\theta$ , which induces a conditional policy  $\pi_\theta(R | \mathcal{I})$  that generates  $\mathcal{R}$  in an autoregressive manner. In this work, we adapt  $\mathcal{M}_\theta$  in two stages: first, we refine the text generation policy using verifiable and clinical textual rewards; second, we further align the model with image-conditioned visual rewards derived from a frozen domain expert, encouraging reports whose disease findings are grounded in the underlying X-ray  $\mathcal{I}$ .

**RRG Objective.** Radiology Report Generation refers to the generation of structured, coherent, and medically informed text from a medical image. In this work, we follow existing works and process the existing report in two parts: the FINDINGS and IMPRESSION sections, where the former contains the broad rationale behind the generated report and the latter contains the potential diseases present in the patient’s medical image. Formally, this process can be represented as follows: given the medical image  $\mathcal{I}$ , the Med-VLM  $\mathcal{M}(\cdot)$  is tasked with interpreting the image, reasoning about it, and generating a descriptive report  $\mathcal{R} = \{r_1, r_2, \dots, r_T\}$  where  $T$  represents the total length of the report and  $r_t \in \mathbb{V}$  represents the tokens in the vocabulary. The report  $\mathcal{R}$  is auto-regressively generated as,

$$p(\mathcal{R} | \mathcal{I}) = \prod_{t=1}^T p(r_t | r_1, \dots, r_{t-1}, \mathcal{I}). \quad (1)$$

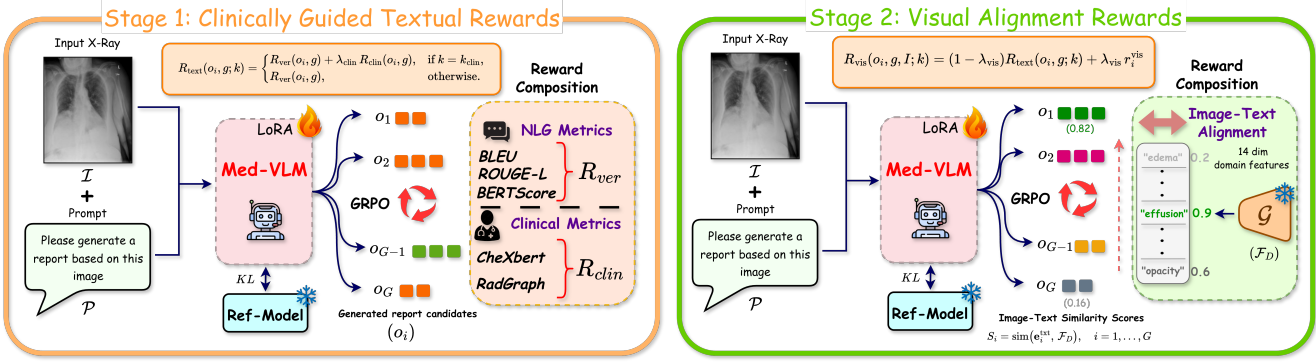


Figure 3. **Workflow of VALOR.** **Left:** In Stage-1, VALOR is trained with verifiable textual rewards  $R_{\text{ver}}$  with periodic clinical guidance  $R_{\text{clin}}$  every  $k_{\text{clin}}$  policy steps to familiarize the base Med-VLM  $\mathcal{M}(\cdot)$  [27] with radiology reasoning patterns. **Right:** In Stage-2, VALOR is further optimized with rewards aligned using *image-text similarity scores* computed by using embeddings obtained utilizing the multi-label domain expert model  $\mathcal{G}$  [21], shifting the model’s reasoning focus from textual knowledge, to grounded, region-wise disease reasoning capabilities. We also utilize `format` rewards to maintain structure of generated reports using `<report>` tags.

## 4. Methodology

### 4.1. On-Policy Learning Framework

Following previous works that applied Group Relative Proximal Optimization (GRPO) to improve the reasoning abilities of medical-VLMs, we use it to improve the reasoning of the base Med-VLM for the task of radiology report generation. GRPO [40] is an algorithm similar to Proximal Policy Optimization (PPO) [38] but with two major differences: (1) Unlike PPO, it does not require a trained reward model for calculating the advantages; instead, it relies on group-relative rewards using generalized advantage estimation (GAE), and (2) it can utilize verifiable rule-based outcomes as rewards, which can be as simple as the metrics used for benchmarking and evaluation. At each alignment step, the Med-VLM  $\mathcal{M}(\cdot)$  rolls out a set of candidate responses  $\{o_i\}_{i=1}^G$  from the current policy  $\pi_{\theta_{\text{old}}}$  and each candidate output is assigned a scalar reward  $r_i$  at the two stages of the optimization process. The advantages  $A_i$  are calculated using the group-relative mean and standard-deviations of the batch  $G$ ,

$$A_i = \frac{r_i - \text{mean}(\{r_j\}_{j=1}^G)}{\text{std}(\{r_j\}_{j=1}^G)}. \quad (2)$$

Therefore, the GRPO objective is given as,

$$\mathcal{L}_{\text{GRPO}}(\theta) = -\frac{1}{G} \sum_{i=1}^G \frac{1}{|o_i|} \sum_{t=1}^{|o_i|} \min(r_{i,t}(\theta) \hat{A}_{i,t}, \text{clip}(r_{i,t}(\theta), 1 - \epsilon, 1 + \epsilon) \hat{A}_{i,t}) - \beta D_{\text{KL}}[\pi_{\theta} \parallel \pi_{\text{ref}}] \quad (3)$$

with  $r_{i,t}(\theta) = \frac{\pi_{\theta}(o_{i,t}|q, o_{i,<t})}{\pi_{\theta_{\text{old}}}(o_{i,t}|q, o_{i,<t})}$  and where  $D_{\text{KL}}(\pi_{\theta} \parallel \pi_{\text{ref}})$  serves as a regularization term penalizing divergence from the reference policy  $\pi_{\text{ref}}$ , with  $\beta$

controlling its regularization strength of the policy.

### 4.2. Supervised Fine-Tuning

Before RL-tuning, we perform a supervised fine-tuning (SFT) phase to adapt  $\mathcal{M}(\cdot)$  to the radiology report generation task following existing works, where SFT is carried out on curated data to improve base-reasoning and stabilize subsequent RL-based optimization [43, 59]. Given the SFT dataset  $\mathcal{D}_{\text{sft}} = \{(I, \mathcal{R}_{\text{sft}})\}$  of chest X-rays  $I$ , prompts  $P$ , and expert reports  $\mathcal{R}_{\text{sft}}$ , we update the model parameters of  $\mathcal{M}(\cdot)$  by minimizing the negative log-likelihood w.r.t ground-truth tokens,

$$\mathcal{L}_{\text{SFT}}(\theta) = \mathbb{E}_{(I, \mathcal{R}_{\text{sft}}) \sim \mathcal{D}} \left[ -\sum_{t=1}^T \log \pi_{\theta}(r_t^{\text{sft}} \mid I, r_{<t}^{\text{sft}}) \right] \quad (4)$$

where  $\mathcal{R}_{\text{sft}} = (r_1^{\text{sft}}, \dots, r_T^{\text{sft}})$  denotes the tokenized report, and  $\pi_{\theta}$  is the conditional distribution induced by  $\mathcal{M}(\cdot)$ . This SFT warmup teaches the model to respect the report structure and produce structurally well-formed reports conditioned on the input image  $I$  and prompt  $P$ . In practice, we find that starting from an SFT checkpoint leads to faster convergence and avoids degenerate “cold-start” tokens. This SFT fine-tuned policy  $\pi_{\theta}$  is then further trained using our multistage reward policy described below.

### 4.3. Multi-Stage Rewards for Visual Alignment

To guide the policy toward radiology knowledge and visually grounded outputs, we design a multi-tier reward system. The first phase focuses on semantic alignment, format adherence, and clinical accuracy using textual rewards, whereas the second phase emphasizes image–text alignment between the generated report and input image, injecting disease-relevant visual reasoning.

---

**Algorithm 1** **VALOR**: Multi-Stage Visual Alignment

---

**Require:** Dataset  $\mathcal{D} = \{(I, \mathcal{R}_{\text{gt}})\}$ , Med-VLM  $\mathcal{M}_\theta$ , frozen expert  $\mathcal{G}$ , group size  $G$

# SFT and frozen reference

$$\theta \leftarrow \theta_{\text{SFT}}, \quad \theta_{\text{ref}} \leftarrow \theta, \quad k \leftarrow 0$$

for  $t \in \{0, 1\}$  do  $t=0: \text{text}; t=1: \text{text+visual}$

- Configure trainable modules of  $\mathcal{M}_\theta$  for stage  $t$
- for minibatch  $B \subset \mathcal{D}$  do

  - $k \leftarrow k + 1$
  - for each  $(I, \mathcal{R}_{\text{gt}}) \in B$  do

    - Sample candidates  $\{o_i\}_{i=1}^G \sim \pi_\theta(\cdot | I, P)$
    - # Stage-1 rewards (Eq. (7))
    - $R_{\text{ver}}(o_i, \mathcal{R}_{\text{gt}}) \leftarrow$

BLEU-4, ROUGE-L, BERTScore

$R_{\text{clin}}(o_i, \mathcal{R}_{\text{gt}}) \leftarrow s_{\text{cx}}, s_{\text{rg}}$

$R_{\text{text}}(o_i; k) \leftarrow R_{\text{ver}} + [k=k_{\text{clin}}] \lambda_{\text{clin}} R_{\text{clin}}$

if  $t=1$  then

- # Img-text consistency (Eqn. (8)–(10))
- $F_D \leftarrow \mathcal{G}_{\text{img}}(I), \quad e_i \leftarrow \mathcal{G}_{\text{txt}}(o_i)$
- $s_i \leftarrow \text{sim}(e_i, F_D), \quad r_i^{\text{vis}} \leftarrow 1 - \text{rank}(S_i) - 1$
- $z - 1$
- $R_{\text{vis}}(o_i; k) \leftarrow (1 - \lambda_{\text{vis}}) R_{\text{text}}(o_i; k) + \lambda_{\text{vis}} r_i^{\text{vis}}$
- $A_i \leftarrow \text{RankNorm}(\{R_{\text{vis}}(o_j; k)\}_{j=1}^G)$
- else
- $A_i \leftarrow \text{RankNorm}(\{R_{\text{text}}(o_j; k)\}_{j=1}^G)$

# GRPO policy update w. KL to reference

$\theta \leftarrow \text{GRPO}(\theta; \{(o_i, A_i)\}_{i=1}^G, \pi_{\theta_{\text{ref}}})$

return  $\mathcal{M}_{\theta^*}$

---

**Clinically-Guided Textual Reward.** In Stage-1 ( $t=0$ ), we adapt the Med-VLM using *verifiable* text rewards that can be computed directly from the ground-truth report. We combine sentence-level BLEU-4 and ROUGE-L, which emphasize report token similarity, with BERTScore, which measures semantic similarity while being less sensitive to generic template text. In addition, we enforce a simple tag-based schema reward to discourage format violations.

$$R_{\text{ver}}(o_i, g) = \lambda_{\text{lex}} [\text{BLEU}_4(o_i, g) + \text{ROUGE}_L(o_i, g)] + \lambda_{\text{sem}} \text{BERTScore}(o_i, g), \quad (5)$$

where  $\lambda_{\text{lex}}, \lambda_{\text{sem}} \geq 0$  and  $\lambda_{\text{lex}} + \lambda_{\text{sem}} = 1$ .

To encourage clinically correct disease terms, we use the micro-averaged F1 scores from CheXbert and RadGraph entities as *periodic* rewards. Let  $s_{\text{cx}}, s_{\text{rg}} \in [0, 1]$  denote normalized F1 scores between labels (or triples) and entities extracted from  $o$  and  $g$ . We define the clinical reward as,

$$R_{\text{clin}}(o_i, g) = \lambda_{\text{cx}} s_{\text{cx}}(o_i, g) + \lambda_{\text{rg}} s_{\text{rg}}(o_i, g), \quad (6)$$

with  $\lambda_{\text{cx}}, \lambda_{\text{rg}} \geq 0$  as weighting hyperparameters.

Rather than applying clinical rewards at every policy step, which can destabilize the optimization, we inject them only every  $k_{\text{clin}}$  updates. Let  $k$  denote the global policy update step. Then, the Stage-1 scalar reward used to compute group-relative advantages is,

$$R_{\text{text}}(o_i, g; k) = \begin{cases} R_{\text{ver}}(o_i, g) + \lambda_{\text{clin}} R_{\text{clin}}(o_i, g), & \text{if } k = k_{\text{clin}}, \\ R_{\text{ver}}(o_i, g), & \text{otherwise,} \end{cases} \quad (7)$$

where  $\lambda_{\text{clin}} \geq 0$  controls the strength of the periodic clinical contribution. This design provides dense, verifiable supervision at every step while periodically nudging the policy toward clinically faithful language without allowing sparse natural language signals to dominate training.

**Visual-Alignment Reward.** In Stage-2 ( $t=1$ ), we introduce image-text similarity scores that explicitly tie each candidate report to the input X-Ray. For an image  $I$ , we obtain a continuous domain feature vector  $\mathcal{F}_D = \mathcal{G}_{\text{img}}(I)$  from the frozen expert model  $\mathcal{G}$ , and for each sampled candidate  $o_i$ , we compute a text embedding  $\mathbf{e}_i^{\text{txt}} = \mathcal{G}_{\text{txt}}(o_i)$  in the same space as above. We then define the image-text similarity score for each candidate  $i$ ,

$$S_i = \text{sim}(\mathbf{e}_i^{\text{txt}}, \mathcal{F}_D), \quad i = 1, \dots, G, \quad (8)$$

where  $\text{sim}(\cdot, \cdot)$  denotes cosine similarity, and a larger  $S_i$  indicates a stronger agreement between the report and disease-relevant visual features.

To obtain a scale-free visual signal, we convert these scores into rank-normalized visual rewards. Let  $\text{rank}(S_i)$  return 1 for the largest similarity and  $z$  for the smallest; we define

$$r_i^{\text{vis}} = 1 - \frac{\text{rank}(S_i) - 1}{z - 1}, \quad (9)$$

so that  $r_i^{\text{vis}} \in [0, 1]$  assigns the highest score to the most image-consistent candidate within each group.

We retain the scalar textual reward  $R_{\text{text}}(o_i, g; k)$  from Eq. (7), and then define the composite visual-alignment reward,

$$R_{\text{vis}}(o_i, g, I; k) = (1 - \lambda_{\text{vis}}) R_{\text{text}}(o_i, g; k) + \lambda_{\text{vis}} r_i^{\text{vis}} \quad (10)$$

where  $\lambda_{\text{vis}} \in [0, 1]$  acts as the mixing coefficient that controls the strength of visual grounding. The group-relative advantages are then obtained by rank-normalization over this composite reward,

$$A_i^{\text{vis}} = \text{RankNorm}(\{R_{\text{vis}}(o_j, g, I; k)\}_{j=1}^G). \quad (11)$$

Thus, we simply replace Stage-1 advantages with  $A_i^{\text{vis}}$ , which biases the policy toward candidates that are both textually faithful and visually aligned with the input image.

**Format Reward.** To ensure that the generated candidate reports follow the proper format, we impose a format reward

(denoted as  $R_{format}$ ) in both stages to check whether the generated report contains the required tag. Specifically, the report content must be contained within the `<report>` and `</report>` tags, respectively.

## 5. Experiments

### 5.1. Datasets

**IU X-ray.** Indiana University Chest X-Ray (IU-XRay) [12] collection contains 7470 chest X-ray images and 3955 corresponding paired reports. Each report is linked to a frontal (AP/PA) or lateral image projection. Following existing works [59], we follow the standard 7:1:2 split.

**MIMIC-CXR.** MIMIC-CXR [24] is one of the most extensive datasets, containing 227, 835 radiology reports from patients at the Beth Israel Deaconess Medical Center. In this work, we follow the standard convention of official train and test splits in line with the baseline methods [59] to ensure fairness in all evaluations.

### 5.2. Experimental Settings

**Evaluation Metrics.** Following existing works [8, 9, 47], we use the 14 CheXpert [41] labels to assess the clinical accuracy of the generated reports. In addition, we employ commonly used natural language metrics, such as BLEU Score [34], ROUGE [30] and METEOR [13] to assess the quality of the generated reports.

**Benchmarks.** We adopt the experimental settings and benchmarks as in MMedPO [59], evaluating the accuracy and generation quality on the test splits of the IU-XRay [12] and MIMIC-CXR [24].

**Baselines and Implementation Details.** We follow the same comparison protocol as in MMedPO [59] and compare it with Direct Preference Optimization (DPO) [37] a variant of preference optimization, as well as GRPO [40] without any visual alignment, as outlined in Stage-1. We use LLaVa-Medv1.5 [27] as our baseline Med-VLM, in line with other existing methods [59]. We also compare our method on clinical accuracy against MMedPO [59] and RADAR [16] using ground truth labels across 14 disease categories, evaluating precision, recall, and F-1 score. We also compare our method with SOTA proprietary models such as GPT-4o [20] and MAIRA-2 for generation quality. For the GRPO fine-tuning stage, we utilize LoRA fine-tuning [17] with a batch size of 8, a learning rate of  $1e-6$ , and perform the alignment operation for three epochs. Further details on the benchmarking and implementation are included in the Supplementary.

### 5.3. Comparison with State-of-the-Art Methods

**Clinical Reasoning and Generation Quality.** We highlight how VALOR can significantly generate more visually aligned and clinically enriched reports in Figure 4, w.r.t

the baseline Med-VLM (LLaVA-Med [27]) and the ground truth report. Note that VALOR, despite not using any externally trained model or curated medical preferences, is still able to capture the disease-relevant portions of the X-ray (top row) and is able to correctly capture the disease observations (such as “atelectasis,” “cardiomegaly,” “edema,” etc.). In the second row, LLaVA-Med not only hallucinated disease observations that had no correlation with the input image but also generated generic text with no medical terminology. VALOR without the visual alignment performs significantly better than the base med-vlm but still fails in cases where the semantic knowledge of disease prevalent regions is needed. In contrast, VALOR generates reports with disease-relevant observations that closely align with the input X-ray, demonstrating superior clinical reasoning abilities.

**Visual Reasoning and Grounding Abilities.** We also visualize which portions of the image are being focused on by each baseline in Figure 5 by visualizing the gradient overlay of each model on the X-ray. Clearly, it can be seen that not only LLaVA-Med fails to focus on disease-relevant areas, but it also looks at regions that have no bearing on where the potential diseases can be, leading to inaccurate diagnoses, i.e. “no visible abnormalities.” Stage-1 fine-tuned VALOR performs relatively better and is able to detect the opacity in the right lung, but the greater focus on the left lung and pelvis region underlines the insufficient anatomical knowledge in the model. After performing visual alignment, the region where VALOR focuses on becomes much more concentrated and accurate, which is reflected in the generated report which has the correct observations in this context “opacity”, “atelectasis”, and “consolidation.”

**Quantitative Analysis.** We evalaute VALOR prmarily on two tasks: generation quality and clinical accuracy on the two radiology report benchmarks IU-XRay [12] and MIMIC-CXR [24], outperforming state-of-the-art preference tuning method MMedPO [59], DPO [37] and VALOR with only Stage-1 alignment in Table 1. We obtain a significant improvement over MMedPO on all three natural language metrics and VALOR w/ visual alignment. To assess clinical accuracy, we further report CheXpert-based disease accuracy in Table 2. On IU-Xray, VALOR achieves the best F-1 score (57.2%), outperforming RADAR [16] (52.4%) and clearly improving over LLaVA-Med (38.6%) and MMedPO (49.8%). As it can be seen from the overall NLG metrics, the alignment step of our model is crucial for obtaining a large improvement on both the MIMIC-CXR and IU-Xray datasets. Overall, these results demonstrate that VALOR not only produces more fluent and semantically aligned reports but also maintains strong clinical accuracy, establishing a new state of the art despite not using any curated preference data, trained retrieval models, or databases.

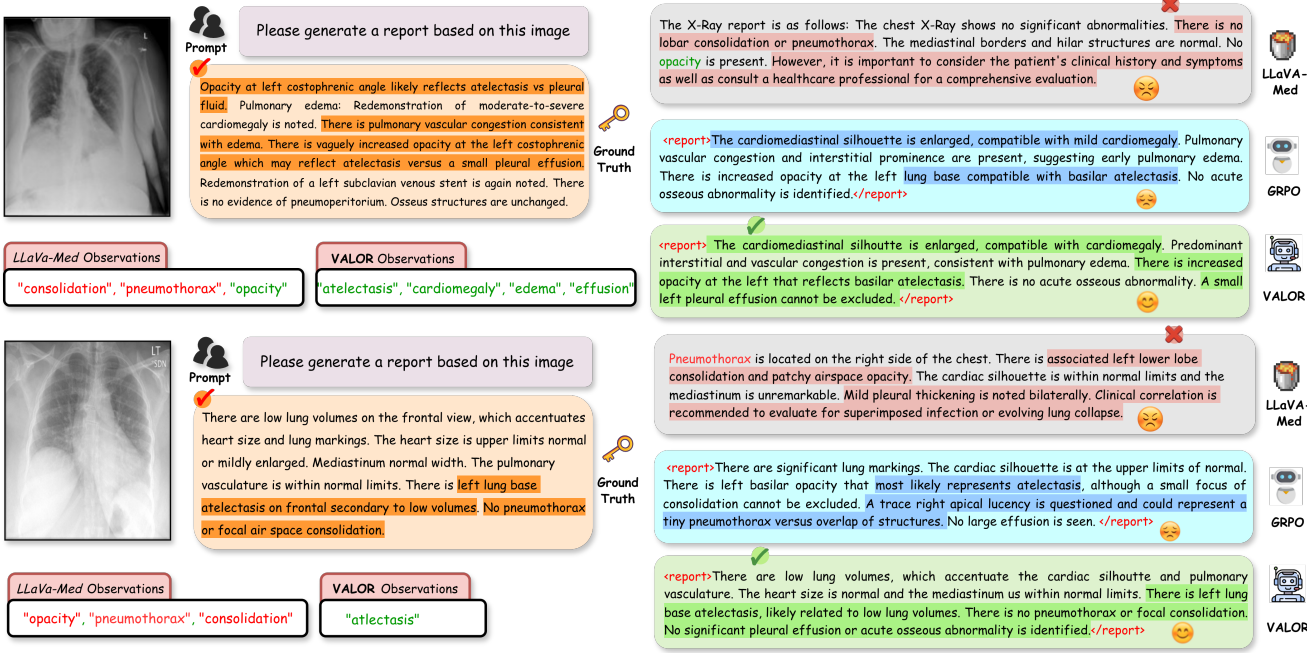


Figure 4. **Generated responses with VALOR.** **Top Row:** LLaVA-Med [27] fails to detect subtle reasoning patterns needed for accurate diagnosis, resulting in hallucination of disease observations such as ‘‘consolidation’’. In contrast, VALOR with verifiable guidance leads to significantly better reasoning and diagnosis capabilities. After Stage-2, VALOR’s visual enhanced reasoning leads to correctly diagonalizing all observations showcasing the need for awareness of disease-relevant portions and sustained attention. **Bottom Row:** LLaVA-Med again hallucinates diseases due to insufficient visual focus, in comparison VALOR reduces hallucinations and generates reports faithful to the X-Ray exhibiting better anatomical and semantic awareness.

Table 1. Detailed performance comparison on the report generation task covering IU-Xray and MIMIC-CXR datasets. BL denotes BLEU. We compare against the following baselines: LLaVa-Med [27], SFT, DPO [37] w/ MMedPO [59] and GRPO [40] on natural language generation quality and coherence.

Models	IU-Xray						MIMIC-CXR					
	BL-1	BL-2	BL-3	BL-4	ROUGE-L	METEOR	BL-1	BL-2	BL-3	BL-4	ROUGE-L	METEOR
LLaVA-Medv1.5	22.29	7.95	2.90	1.05	7.58	4.56	9.62	3.66	1.48	0.63	9.42	5.62
+ SFT	38.42	13.40	4.74	1.67	10.31	10.95	29.41	10.19	3.58	1.26	9.38	7.71
+ DPO [37]	41.63	15.13	5.56	2.03	12.95	17.13	29.61	10.29	3.61	1.27	9.45	7.81
+ MMedPO [59]	55.58	23.93	10.36	4.40	29.52	34.16	31.37	10.93	4.26	1.52	<b>10.96</b>	9.88
+ GRPO [40]	59.02	26.50	11.80	5.10	31.80	35.90	34.10	11.80	4.25	1.45	10.30	9.65
<b>+ VALOR</b>	<b>61.20</b>	<b>28.30</b>	<b>12.90</b>	<b>5.70</b>	<b>33.10</b>	<b>36.88</b>	<b>35.60</b>	<b>12.40</b>	<b>4.55</b>	<b>1.55</b>	10.85	<b>9.95</b>

## 5.4. Ablation Studies

**Comparison with multimodal LLMs.** We also compare our model with mainstream proprietary multimodal LLMs such as GPT-4o [20] and SOTA medical LLM MAIRA-2 [3] in a zero-shot setting in Table 3. Our method outperforms GPT-4o [20] by 17% and MAIRA-2 [3] by an average margin of 5% across the NLG metrics. Therefore, VALOR consistently performs better than both general-purpose and medical multimodal LLMs, showing more anatomy of visual knowledge along with enhanced clinical accuracy despite the significantly larger pre-training knowledge corpus

of these models on large amounts of data.

**Effect of clinical and visual guidance.** In Figure 6, on the left, we ablate the Stage-2 mixing weight  $\lambda_{\text{vis}}$  Eq. (10): BLEU-4, ROUGE-L, and CheXbert F1 peak for  $\lambda_{\text{vis}} \in [0.4, 0.6]$ . Small values under-use visual evidence (mimicking Stage-1), whereas large values overweight similarity and erode fluency, indicating a balance between  $R_{\text{text}}$  and the rank-normalized visual advantage. Figure 6 examines the clinical reward period  $k_{\text{clin}}$ : too frequent signals (small  $k_{\text{clin}}$ ) destabilize training and bias toward terse mentions; too infrequent (large  $k_{\text{clin}}$ ) under-leverages Stage 1 guid-

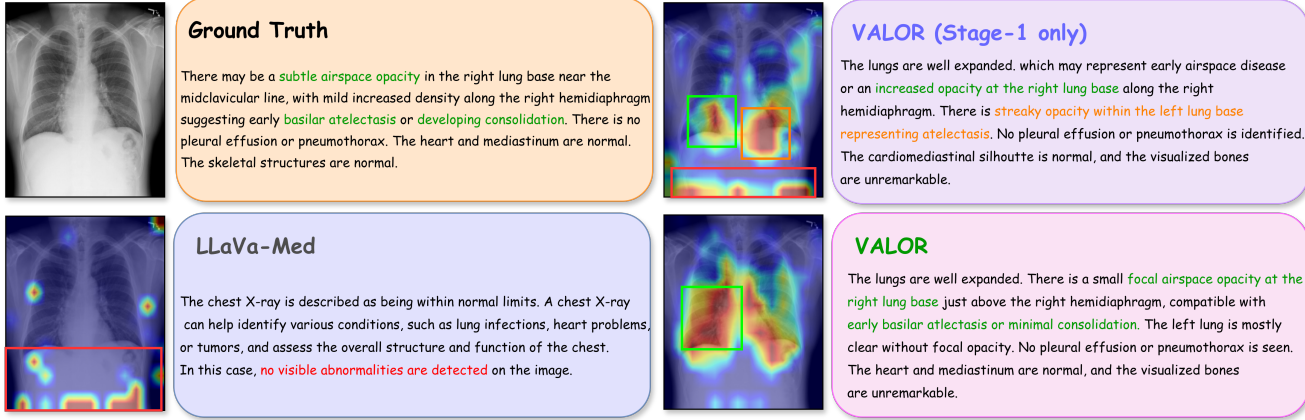


**Figure 5. Attention Map Visualization.** For the input X-Ray  $\mathcal{I}$ , we visualize the specific areas the Med-VLM [27] and VALOR focuses on while generating the report. **Bottom Left:** is the attention map for LLaVA-Med [27] which misses the lung region due to lack of anatomical reasoning, leading to the generated report containing the inaccurate conclusion that no diseases can be detected. **Upper Right:** is the attention map with Stage-1 results of VALOR. It can be seen that it specifically learns to spot the clinically relevant regions for generating the report but still seems to focus on non-important regions at the base of the X-Ray. **Bottom Right:** In comparison, VALOR allocates more attention on the right lung region, the most important area for this particular X-Ray demonstrating better visual localization and reasoning capabilities. <report> tags are omitted here for clarity.

**Table 2. CheXbert disease classification metrics (F1) on the IU-Xray dataset.** Scores are computed using the CheXpert label set diseases; higher values indicate better alignment with expert disease labels.

Model	Precision $\uparrow$	Recall $\uparrow$	F1 $\uparrow$
LLaVA-Med v1.5	40.6	38.4	38.6
MMedPO [59]	47.2	48.6	49.8
RADAR [16]	51.2	52.6	52.4
<b>VALOR</b>	<b>56.6</b>	<b>57.8</b>	<b>57.2</b>

**Table 3. Zero-shot comparison for the report generation task on the IU-Xray [12] dataset against state-of-the-art multimodal medical and non-medical LLMs. Avg BL refers to the mean BLEU score.**

Type	Models	Avg BL $\uparrow$	ROUGE-L $\uparrow$	METEOR $\uparrow$
General VLM	GPT-4o [20]	15.32	18.80	11.50
	<b>VALOR</b>	<b>27.02</b>	<b>33.10</b>	<b>36.88</b>
Medical VLM	MAIRA-2 [3]	20.22	30.60	32.36
	<b>VALOR</b>	<b>27.02</b>	<b>33.10</b>	<b>36.88</b>

ance. A moderate  $k_{\text{clin}}$  yields the best trade-off, as shown in Figure 6. Overall, Stage-1 builds verifiable, clinically consistent text with *periodic* supervision, whereas Stage-2 strengthens visual grounding by *mixing* visual advantages at each policy optimization step.

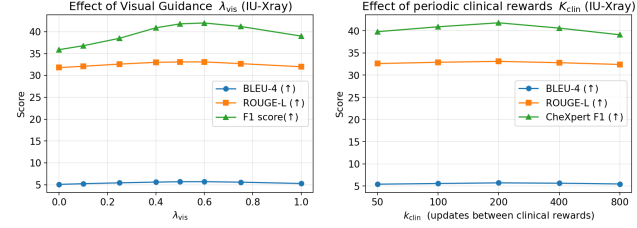


**Figure 6. Evolution of Clinical and visual periodic guidance.** *Left:* VALOR performs better with an optimal value of  $\lambda_{\text{vis}} \sim 0.5$ . *Right:* VALOR performs better with periodic injection of clinical rewards  $R_{\text{clin}}$  per  $k_{\text{clin}}$  steps instead of frequent (per-step) guidance which destabilizes performance.

## 6. Conclusion

We introduced VALOR, a novel multimodal alignment framework that enhances the clinical and visual reasoning capabilities of Medical VLMs. To this end, we propose an alignment framework which utilizes both textual and visual rewards for optimization thereby enhancing the model’s medical multimodal comprehension capabilities. Our results demonstrate the versatility of VALOR across a diverse set of datasets. Further our visualization studies show the effectiveness of our alignment approach, highlighting the crucial role the image plays in the overall task of radiology report generation. Our findings show VALOR’s potential to advance medical image understanding and clinical healthcare. Future work will include more ablations on reward shaping and curriculum schedules to clarify which components drive gains and to mitigate reward hacking. These directions chart a practical path toward image-faithful, clinically reliable report generation systems.

## References

[1] Elmira Amirloo, Jean-Philippe Fauconnier, Christoph Roesmann, Christian Kerl, Rinu Boney, Yusu Qian, Zirui Wang, Afshin Dehghan, Yinfai Yang, Zhe Gan, et al. Understanding alignment in multimodal llms: A comprehensive study. *arXiv preprint arXiv:2407.02477*, 2024. 2

[2] Shruthi Bannur, Stephanie Hyland, Qianchu Liu, Fernando Perez-Garcia, Maximilian Ilse, Daniel C Castro, Benedikt Boecking, Harshita Sharma, Kenza Bouzid, Anja Thieme, et al. Learning to exploit temporal structure for biomedical vision-language processing. In *Proceedings of the IEEE/CVF Conference on Computer Vision and Pattern Recognition*, pages 15016–15027, 2023. 3

[3] Shruthi Bannur, Kenza Bouzid, Daniel C Castro, Anton Schwaighofer, Anja Thieme, Sam Bond-Taylor, Maximilian Ilse, Fernando Pérez-García, Valentina Salvatelli, Harshita Sharma, et al. Maira-2: Grounded radiology report generation. *arXiv preprint arXiv:2406.04449*, 2024. 7, 8

[4] Benedikt Boecking, Naoto Usuyama, Shruthi Bannur, Daniel C Castro, Anton Schwaighofer, Stephanie Hyland, Maria Wetscherek, Tristan Naumann, Aditya Nori, Javier Alvarez-Valle, et al. Making the most of text semantics to improve biomedical vision–language processing. In *European conference on computer vision*, pages 1–21. Springer, 2022. 3

[5] Jianjian Cao, Peng Ye, Shengze Li, Chong Yu, Yansong Tang, Jiwen Lu, and Tao Chen. Madtp: Multi-modal alignment-guided dynamic token pruning for accelerating vision-language transformer. In *Proceedings of the IEEE/CVF conference on computer vision and pattern recognition*, pages 15710–15719, 2024. 2

[6] Junying Chen, Chi Gui, Ruyi Ouyang, Anningzhe Gao, Shunian Chen, Guiming Hardy Chen, Xidong Wang, Ruifei Zhang, Zhenyang Cai, Ke Ji, et al. Huatuogpt-vision, towards injecting medical visual knowledge into multimodal llms at scale. *arXiv preprint arXiv:2406.19280*, 2024. 2, 3

[7] Jiawei Chen, Dingkang Yang, Tong Wu, Yue Jiang, Xiaolu Hou, Mingcheng Li, Shunli Wang, Dongling Xiao, Ke Li, and Lihua Zhang. Detecting and evaluating medical hallucinations in large vision language models. *arXiv preprint arXiv:2406.10185*, 2024. 2

[8] Zihong Chen, Yan Song, Tsung-Hui Chang, and Xiang Wan. Generating radiology reports via memory-driven transformer. *arXiv preprint arXiv:2010.16056*, 2020. 6

[9] Zihong Chen, Yaling Shen, Yan Song, and Xiang Wan. Cross-modal memory networks for radiology report generation. *arXiv preprint arXiv:2204.13258*, 2022. 6

[10] Yun-Wei Chu, Kai Zhang, Christopher Malon, and Martin Renqiang Min. Reducing hallucinations of medical multimodal large language models with visual retrieval-augmented generation. In *Workshop on Large Language Models and Generative AI for Health at AAAI*, 2025. 3

[11] Hejie Cui, Lingjun Mao, Xin Liang, Jieyu Zhang, Hui Ren, Quanzheng Li, Xiang Li, and Carl Yang. Biomedical visual instruction tuning with clinician preference alignment. *Advances in neural information processing systems*, 37:96449–96467, 2024. 2

[12] Dina Demner-Fushman, Marc D Kohli, Marc B Rosenman, Sonya E Shooshan, Laritza Rodriguez, Sameer Antani, George R Thoma, and Clement J McDonald. Preparing a collection of radiology examinations for distribution and retrieval. *Journal of the American Medical Informatics Association*, 23(2):304–310, 2015. 2, 6, 8

[13] Michael Denkowski and Alon Lavie. Meteor 1.3: Automatic metric for reliable optimization and evaluation of machine translation systems. In *Proceedings of the sixth workshop on statistical machine translation*, pages 85–91, 2011. 2, 6

[14] Guanting Dong, Yutao Zhu, Chenghao Zhang, Zechen Wang, Ji-Rong Wen, and Zhicheng Dou. Understand what llm needs: Dual preference alignment for retrieval-augmented generation. In *Proceedings of the ACM on Web Conference 2025*, pages 4206–4225, 2025. 3

[15] Sepp Hochreiter and Jürgen Schmidhuber. Long short-term memory. *Neural computation*, 9(8):1735–1780, 1997. 3

[16] Wenjun Hou, Yi Cheng, Kaishuai Xu, Heng Li, Yan Hu, Wenjie Li, and Jiang Liu. RADAR: Enhancing radiology report generation with supplementary knowledge injection. In *Proceedings of the 63rd Annual Meeting of the Association for Computational Linguistics (ACL)*, 2025. 2, 3, 6, 8

[17] Edward J Hu, Yelong Shen, Phillip Wallis, Zeyuan Allen-Zhu, Yuanzhi Li, Shean Wang, Lu Wang, Weizhu Chen, et al. Lora: Low-rank adaptation of large language models. *ICLR*, 1(2):3, 2022. 6

[18] Qidong Huang, Xiaoyi Dong, Pan Zhang, Bin Wang, Conggui He, Jiaqi Wang, Dahua Lin, Weiming Zhang, and Nenghai Yu. Opera: Alleviating hallucination in multi-modal large language models via over-trust penalty and retrospection-allocation. In *Proceedings of the IEEE/CVF Conference on Computer Vision and Pattern Recognition (CVPR)*, pages 13418–13427, 2024. 2

[19] Zhongzhen Huang, Xiaofan Zhang, and Shaotong Zhang. Kiut: Knowledge-injected u-transformer for radiology report generation. In *Proceedings of the IEEE/CVF conference on computer vision and pattern recognition*, pages 19809–19818, 2023. 3

[20] Aaron Hurst, Adam Lerer, Adam P Goucher, Adam Perelman, Aditya Ramesh, Aidan Clark, AJ Ostrow, Akila Welihinda, Alan Hayes, Alec Radford, et al. Gpt-4o system card. *arXiv preprint arXiv:2410.21276*, 2024. 6, 7, 8

[21] Jeremy Irvin, Pranav Rajpurkar, Michael Ko, Yifan Yu, Silvana Ciurea-Ilcus, Chris Chute, Henrik Marklund, Behzad Haghgoor, Robyn Ball, Katie Shpanskaya, et al. Chexpert: A large chest radiograph dataset with uncertainty labels and expert comparison. In *Proceedings of the AAAI conference on artificial intelligence*, pages 590–597, 2019. 2, 4

[22] Saahil Jain, Ashwin Agrawal, Adriel Saporta, Steven QH Truong, Du Nguyen Duong, Tan Bui, Pierre Chambon, Yuhao Zhang, Matthew P Lungren, Andrew Y Ng, et al. Radgraph: Extracting clinical entities and relations from radiology reports. *arXiv preprint arXiv:2106.14463*, 2021. 2, 3

[23] Haibo Jin, Haoxuan Che, Yi Lin, and Hao Chen. Promptmrg: Diagnosis-driven prompts for medical report generation. In *Proceedings of the AAAI Conference on Artificial Intelligence*, pages 2607–2615, 2024. 3

[24] Alistair Johnson, Lucas Bulgarelli, Tom Pollard, Steven Horng, Leo Anthony Celi, and Roger Mark. Mimic-iv. *PhysioNet*. Available online at: <https://physionet.org/content/mimiciv/1.0/> (accessed August 23, 2021), pages 49–55, 2020. 2, 6

[25] Sicong Leng, Hang Zhang, Guanzheng Chen, Xin Li, Shijian Lu, Chunyan Miao, and Lidong Bing. Mitigating object hallucinations in large vision-language models through visual contrastive decoding. In *Proceedings of the IEEE/CVF Conference on Computer Vision and Pattern Recognition*, pages 13872–13882, 2024. 2

[26] Bin Xu Li, Tiankai Yan, Yuanting Pan, Jie Luo, Ruiyang Ji, Jiayuan Ding, Zhe Xu, Shilong Liu, Haoyu Dong, Zihao Lin, et al. Mmedagent: Learning to use medical tools with multi-modal agent. *arXiv preprint arXiv:2407.02483*, 2024. 3

[27] Chunyuan Li, Cliff Wong, Sheng Zhang, Naoto Usuyama, Haotian Liu, Jianwei Yang, Tristan Naumann, Hoifung Poon, and Jianfeng Gao. Llava-med: Training a large language-and-vision assistant for biomedicine in one day. *Advances in Neural Information Processing Systems*, 36:28541–28564, 2023. 1, 2, 4, 6, 7, 8

[28] Mingjie Li, Bingqian Lin, Zicong Chen, Haokun Lin, Xianan Liang, and Xiaojun Chang. Dynamic graph enhanced contrastive learning for chest x-ray report generation. In *Proceedings of the IEEE/CVF Conference on Computer Vision and Pattern Recognition*, pages 3334–3343, 2023. 3

[29] Xinze Li, Sen Mei, Zhenghao Liu, Yukun Yan, Shuo Wang, Shi Yu, Zheni Zeng, Hao Chen, Ge Yu, Zhiyuan Liu, et al. Rag-ddr: Optimizing retrieval-augmented generation using differentiable data rewards. *arXiv preprint arXiv:2410.13509*, 2024. 3

[30] Chin-Yew Lin. Rouge: A package for automatic evaluation of summaries. In *Text summarization branches out*, pages 74–81, 2004. 2, 6

[31] Bo Liu, Ke Zou, Li-Ming Zhan, Zexin Lu, Xiaoyu Dong, Yidi Chen, Chengqiang Xie, Jiannong Cao, Xiao-Ming Wu, and Huazhu Fu. Gemex: A large-scale, groundable, and explainable medical vqa benchmark for chest x-ray diagnosis. In *Proceedings of the IEEE/CVF International Conference on Computer Vision*, pages 21310–21320, 2025. 2

[32] Michael Moor, Qian Huang, Shirley Wu, Michihiro Yasunaga, Yash Dalmia, Jure Leskovec, Cyril Zakka, Eduardo Pontes Reis, and Pranav Rajpurkar. Med-flamingo: a multimodal medical few-shot learner. In *Machine Learning for Health (ML4H)*, pages 353–367. PMLR, 2023. 3

[33] Vishwesh Nath, Wenqi Li, Dong Yang, Andriy Myronenko, Mingxin Zheng, Yao Lu, Zhijian Liu, Hongxu Yin, Yee Man Law, Yucheng Tang, et al. Vila-m3: Enhancing vision-language models with medical expert knowledge. In *Proceedings of the Computer Vision and Pattern Recognition Conference*, pages 14788–14798, 2025. 2, 3

[34] Kishore Papineni, Salim Roukos, Todd Ward, and Wei-Jing Zhu. Bleu: a method for automatic evaluation of machine translation. In *Proceedings of the 40th annual meeting of the Association for Computational Linguistics*, pages 311–318, 2002. 2, 6

[35] Sang-Jun Park, Keun-Soo Heo, Dong-Hee Shin, Young-Han Son, Ji-Hye Oh, and Tae-Eui Kam. Dart: Disease-aware image-text alignment and self-correcting re-alignment for trustworthy radiology report generation. In *Proceedings of the Computer Vision and Pattern Recognition Conference*, pages 15580–15589, 2025. 3

[36] Alec Radford, Jong Wook Kim, Chris Hallacy, Aditya Ramesh, Gabriel Goh, Sandhini Agarwal, Girish Sastry, Amanda Askell, Pamela Mishkin, Jack Clark, et al. Learning transferable visual models from natural language supervision. In *International conference on machine learning*, pages 8748–8763. PMLR, 2021. 3

[37] Rafael Rafailov, Archit Sharma, Eric Mitchell, Christopher D Manning, Stefano Ermon, and Chelsea Finn. Direct preference optimization: Your language model is secretly a reward model. *Advances in neural information processing systems*, 36:53728–53741, 2023. 6, 7

[38] John Schulman, Filip Wolski, Prafulla Dhariwal, Alec Radford, and Oleg Klimov. Proximal policy optimization algorithms. *arXiv preprint arXiv:1707.06347*, 2017. 4

[39] Andrew Sellgren, Sahar Kazemzadeh, Tiam Jaroensri, Atilla Kiraly, Madeleine Traverse, Timo Kohlberger, Shawn Xu, Fayaz Jamil, Cian Hughes, Charles Lau, et al. Medgemma technical report. *arXiv preprint arXiv:2507.05201*, 2025. 2

[40] Zhihong Shao, Peiyi Wang, Qihao Zhu, Runxin Xu, Junxiao Song, Xiao Bi, Haowei Zhang, Mingchuan Zhang, Y. K. Li, Y. Wu, and Daya Guo. Deepseekmath: Pushing the limits of mathematical reasoning in open language models, 2024. 3, 4, 6, 7

[41] Akshay Smit, Saahil Jain, Pranav Rajpurkar, Anuj Pareek, Andrew Y Ng, and Matthew P Lungren. Chexbert: combining automatic labelers and expert annotations for accurate radiology report labeling using bert. *arXiv preprint arXiv:2004.09167*, 2020. 2, 6

[42] Liwen Sun, James Jialun Zhao, Wenjing Han, and Chenyan Xiong. Fact-aware multimodal retrieval augmentation for accurate medical radiology report generation. In *Proceedings of the 2025 Conference of the Nations of the Americas Chapter of the Association for Computational Linguistics: Human Language Technologies (Volume 1: Long Papers)*, pages 643–655, 2025. 2

[43] Zhiqing Sun, Sheng Shen, Shengcao Cao, Haotian Liu, Chunyuan Li, Yikang Shen, Chuang Gan, Liangyan Gui, Yuxiong Wang, Yiming Yang, et al. Aligning large multimodal models with factually augmented rlhf. In *Findings of the Association for Computational Linguistics: ACL 2024*, pages 13088–13110, 2024. 4

[44] Tim Tanida, Philip Müller, Georgios Kaassis, and Daniel Rueckert. Interactive and explainable region-guided radiology report generation. In *Proceedings of the IEEE/CVF Conference on Computer Vision and Pattern Recognition*, pages 7433–7442, 2023. 3

[45] Ekin Tiu, Ellie Talius, Pujan Patel, Curtis P Langlotz, Andrew Y Ng, and Pranav Rajpurkar. Expert-level detection of pathologies from unannotated chest x-ray images via self-supervised learning. *Nature biomedical engineering*, 6(12):1399–1406, 2022. 3

[46] Zifeng Wang, Zhenbang Wu, Dinesh Agarwal, and Jimeng Sun. Medclip: Contrastive learning from unpaired medi-

cal images and text. In *Proceedings of the Conference on Empirical Methods in Natural Language Processing. Conference on Empirical Methods in Natural Language Processing*, page 3876, 2022. 3

[47] Zhenyu Wang, Lingqiao Liu, Lei Wang, and Luping Zhou. Metrtransformer: Radiology report generation by transformer with multiple learnable expert tokens. In *Proceedings of the IEEE/CVF conference on computer vision and pattern recognition*, pages 11558–11567, 2023. 6

[48] Zitian Wang, Yue Liao, Kang Rong, Fengyun Rao, Yibo Yang, and Si Liu. Instruction-oriented preference alignment for enhancing multi-modal comprehension capability of mllms. *arXiv preprint arXiv:2503.20309*, 2025. 3

[49] Chaoyi Wu, Xiaoman Zhang, Ya Zhang, Yanfeng Wang, and Weidi Xie. Medclip: Medical knowledge enhanced language-image pre-training in radiology. *arXiv preprint arXiv:2301.02228*, 2023. 3

[50] Peng Xia, Kangyu Zhu, Haoran Li, Tianze Wang, Weijia Shi, Sheng Wang, Linjun Zhang, James Zou, and Huaxiu Yao. Mmed-rag: Versatile multimodal rag system for medical vision language models. *arXiv preprint arXiv:2410.13085*, 2024. 3

[51] Peng Xia, Kangyu Zhu, Haoran Li, Hongtu Zhu, Yun Li, Gang Li, Linjun Zhang, and Huaxiu Yao. Rule: Reliable multimodal rag for factuality in medical vision language models. *arXiv preprint arXiv:2407.05131*, 2024. 2

[52] Tianyu Yu, Haoye Zhang, Qiming Li, Qixin Xu, Yuan Yao, Da Chen, Xiaoman Lu, Ganqu Cui, Yunkai Dang, Taiwen He, et al. Rlaif-v: Open-source ai feedback leads to super gpt-4v trustworthiness. In *Proceedings of the Computer Vision and Pattern Recognition Conference*, pages 19985–19995, 2025. 3

[53] Kai Zhang, Rong Zhou, Eashan Adhikarla, Zhiling Yan, Yixin Liu, Jun Yu, Zhengliang Liu, Xun Chen, Brian D Davison, Hui Ren, et al. A generalist vision–language foundation model for diverse biomedical tasks. *Nature Medicine*, 30(11):3129–3141, 2024. 3

[54] Sheng Zhang, Yanbo Xu, Naoto Usuyama, Hanwen Xu, Jaspreet Bagga, Robert Tinn, Sam Preston, Rajesh Rao, Mu Wei, Naveen Valluri, et al. Biomedclip: a multimodal biomedical foundation model pretrained from fifteen million scientific image-text pairs. *arXiv preprint arXiv:2303.00915*, 2023. 3

[55] Tianyi Zhang, Varsha Kishore, Felix Wu, Kilian Q Weinberger, and Yoav Artzi. Bertscore: Evaluating text generation with bert. *arXiv preprint arXiv:1904.09675*, 2019. 2

[56] Juexiao Zhou, Xiuying Chen, and Xin Gao. Path to medical agi: Unify domain-specific medical llms with the lowest cost. *arXiv preprint arXiv:2306.10765*, 2023. 2

[57] Juexiao Zhou, Xiaonan He, Liyuan Sun, Jiannan Xu, Xiuying Chen, Yuetan Chu, Longxi Zhou, Xingyu Liao, Bin Zhang, and Xin Gao. Skingpt-4: an interactive dermatology diagnostic system with visual large language model. *arXiv preprint arXiv:2304.10691*, 2023. 2

[58] Yiyang Zhou, Chenhang Cui, Rafael Rafailov, Chelsea Finn, and Huaxiu Yao. Aligning modalities in vision large language models via preference fine-tuning. *arXiv preprint arXiv:2402.11411*, 2024. 2, 3

[59] Kangyu Zhu, Peng Xia, Yun Li, Hongtu Zhu, Sheng Wang, and Huaxiu Yao. Mmedpo: Aligning medical vision-language models with clinical-aware multimodal preference optimization. *arXiv preprint arXiv:2412.06141*, 2024. 2, 3, 4, 6, 7, 8